PHYSICAL REVIEW B **68**, 201307(R) (2003)

Point contact spin spectroscopy of ferromagnetic MnAs epitaxial films

R. P. Panguluri,[1] G. Tsoi,[1] B. Nadgorny,[1] S. H. Chun,[2,3] N. Samarth,[2] and I. I. Mazin[4]
[1]*Department of Physics and Astronomy, Wayne State University, Detroit, Michigan 48201, USA*
[2]*Department of Physics and Materials Research Institute, The Pennsylvania State University, University Park, Pennsylvania 16802, USA*
[3]*Department of Physics, Sejong University, Seoul 143-747, Korea*
[4]*Code 6390, Naval Research Laboratory, 4555 Overlook Ave., Washington D.C. 20375, USA*
(Received 11 June 2003; published 24 November 2003)

We use point contact Andreev reflection spectroscopy to measure the transport spin polarization of MnAs epitaxial films grown on (001) GaAs. By analyzing both the temperature dependence of the contact resistance and the phonon spectra of lead, acquired simultaneously with the spin polarization measurements, we demonstrate that all the contacts are in the ballistic limit. A ballistic transport spin polarization of approximately 49% and 44% is obtained for the type *A* and type *B* orientations of MnAs, respectively. These measurements are consistent with our density functional calculations, and with recent observations of a large tunnel magnetoresistance in MnAs/AlAs/(Ga,Mn)As tunnel junctions.

DOI: 10.1103/PhysRevB.68.201307 PACS number(s): 72.25.Ba, 71.20.Gj, 74.45.+c, 74.50.+r

Contemporary interest in spintronics has recently focused on the injection, transport, and relaxation spin processes in semiconductors and their heterostructures. Unlike all-metal devices, where efficient spin injection has been demonstrated, spin injection from ferromagnetic metals into semiconductors proved to be more challenging, due in part to the small interface resistance, or the ''conductivity mismatch.'' [1] This hurdle can be overcome by spin injection via magnetic semiconductor contacts, fully spin polarized metal (''half-metal'') contacts, or tunnel contacts.[2–4] In this context, it is particularly important to measure the spin polarization in ferromagnets, such as MnAs and (Ga,Mn)As that can be integrated with technologically important semiconductors, GaAs and GaAs-based heterostructures via molecular beam epitaxy (MBE).[5,6] A direct measurement of the spin polarization of MnAs and (Ga,Mn)As is relevant to the understanding of MnAs/AlAs/(Ga,Mn)As junctions that show a large tunnel magnetoresistance ($\sim$30% at $\sim$5 K).[3] While the first spin polarization measurements of (Ga,Mn)As are just emerging,[7] there have been no reported measurements of MnAs, which has a higher ferromagnetic transition temperature (320 K) than (GaMn)As. Furthermore, band structure calculations predict that MnAs can be nearly half-metallic in the hypothetical zinc-blende structure.[8] We note that MnAs is a ferromagnetic metal, and is very different from (Ga,Mn)As in its structural, magnetic, and electronic properties.

The epitaxial growth of MnAs on (001) GaAs can produce two possible crystalline orientations of the NiAs phase, selected by specific growth conditions:[5,6] in ''type *A*'' samples the growth axis is along $[\bar{1}100]$ MnAs and the *c* axis is in the (001) plane of the GaAs substrate, while in ''type *B*'' samples the growth axis is along $[\bar{1}101]$ MnAs planes and the *c* axis is at an angle of $\sim$23° to the plane of the substrate.

Here, we report the results of point contact Andreev reflection (PCAR) measurements of the ballistic transport spin polarization in both type *A* and type *B* ferromagnetic epilayers of MnAs grown on (100) GaAs. The results are consistent with our density functional calculations.

Depending on the experiment, spin polarization can be defined in a number of ways. Our interest here focuses on the *transport* spin polarization that can be often written as $P_n = [N_\uparrow(E_F)V^n_{F\uparrow} - N_\downarrow(E_F)V^n_{F\downarrow}]/[N_\uparrow(E_F)V^n_{F\uparrow} + N_\downarrow(E_F)V^n_{F\downarrow}]$, where $N_\uparrow(E_F)$, $N_\downarrow(E_F)$, and $V_{F\uparrow}$, $V_{F\downarrow}$ are the densities of states and the Fermi velocities for majority and minority spin bands, respectively, and P_1 and P_2 refer to the ballistic and diffusive regimes, respectively. The PCAR technique[9,10] based on Andreev reflection measures the spin polarization of the current in a ferromagnet (F) interfaced with a superconductor (S). For the spin-polarized current, Andreev conductance below the superconducting gap is partially suppressed.[11] The current transfer across the F-S interface can be described in detail,[12] using a generalized Blonder-Tinkham-Klapwijk (GBTK) model[13] for both ballistic (mean free path L is larger than the contact size d) and diffusive ($L<d$) point contacts. Despite many approximations in the derivation of the GBTK formulas[12] (e.g., a δ-function barrier which may not always be adequate for real systems[14]), it often provides a good description of the data, performing well beyond its limit of applicability. For instance, it is known to produce good fits of the data with the interface resistance $Z=0$, although within the BTK model Z can never be equal to zero because of the Fermi velocity mismatch.[14,15] The correct interpretation of the spin polarization measurements also requires a clear identification of the transport regime (diffusive versus ballistic). We establish the transport regime experimentally (see below). Additionally, we measure the *phonon spectra* of the point contact for Pb to evaluate the contact quality.

The Pb and Sn probes for this study were fabricated by fine mechanical polishing of the thin rods.[9] A shaft connected to a differential type screw was used to change the position of the tip by about 10 μm per revolution, allowing good control over the contact resistance with approximately an order of magnitude better sensitivity than in Refs. 9 and 16. After the contact is established, the shaft was disconnected from the sample stage, eliminating most of the temperature gradients and significantly increasing the stability of the contact. This design allowed us to measure the resistance of the

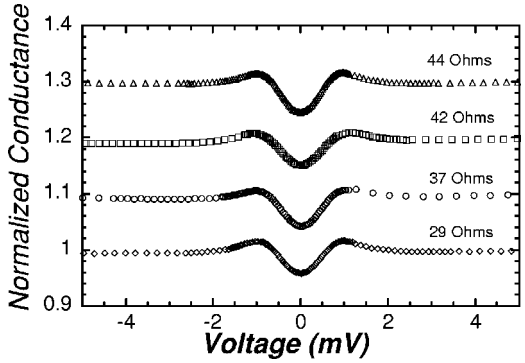

FIG. 1. Normalized conductance of a series of Sn point contacts with different contact resistance R_c (from 29 Ω to 44 Ω) of a type *A* MnAs with at $T=1.2$ K. For convenience, a uniform vertical offset is used for plotting each consecutive curve.

contact in a broad temperature range, allowing independent determination of the mean free path and the contact size. All measurements were made by a four-probe technique, with the differential conductance dI/dV obtained by standard ac lock-in detection at a frequency of ~2 kHz within the temperature range 1.2–4.2 K. The second derivative d^2I/dV^2 was also recorded to obtain the point contact phonon spectra.

The MnAs epilayers with thicknesses between 40 nm and 200 nm were grown in an EPI 930 MBE system using standard solid source effusion cells. The substrate temperature was monitored using a thermocouple situated behind the substrate mounting blocks. The sample growth was monitored using reflection high-energy electron diffraction (RHEED) at 12 keV. All samples were grown on nonvicinal GaAs (001) substrates prepared using *in situ* thermal cleaning under As overpressure. A 100-nm thick GaAs buffer was first grown at 600 °C. Upon cooling in an As overpressure to a substrate temperature of 250 °C, RHEED indicated a $c(4\times4)$ reconstructed GaAs surfaces. Type *A* samples were produced by either directly depositing MnAs on this surface, or on an *annealed* thin layer of low-temperature-grown GaAs (LT-GaAs). In contrast, for type *B* samples, the MnAs layer was deposited on the unreconstructed surface of an unannealed LT-GaAs layer. The magnetic properties of the MnAs films used in this study are comparable to that observed by others,[5,17] with the coercivity along the easy $[11\bar{2}0]$ magnetization axis (~200 Oe) approximately two orders of magnitude lower than the coercivity along the hard [0001] axis (~3 T).

PCAR measurements were carried out on several MnAs type *A* and type *B* samples, with approximately 10 different point contacts measured for each sample using both Sn and Pb superconducting tips. The geometry of the epilayer only permits measurements along the growth axis, $[\bar{1}100]$ for type *A* samples and $[\bar{1}101]$ direction for type *B*. Figure 1 shows several consecutive conductance curves for different Sn contacts to type *A* MnAs sample. The dI/dV characteristics of this series of contacts are very analagous, essentially independent of the contact resistance, thus yielding practically the same values of the spin polarization. The data obtained with the Pb tips is similar. The spin polarization is extracted from the dI/dV data in Fig. 1 using a modified GBTK theory.[12] Since, as it will be shown below, all contacts are clearly in the ballistic regime, we use the ballistic theory to analyze the data. A typical fit of one of the curves from Fig. 1 is shown in Fig. 2(a), while for comparison Fig. 2(b) shows an example of the fit for a superconducting Pb point contact with a type *B* MnAs. For the great majority of the contacts, the barrier strength *Z* turned out to be rather small ($Z\sim0.1-0.15$); see Fig. 2. Thus the question of a possible *Z* dependence of the spin polarization raised recently[18] does not appear relevant for this study.

The average spin polarization obtained for type *A* MnAs is $P\sim(49\pm2)\%$ and for type *B* MnAs$\sim(44\pm4)\%$, which might indicate the presence of the spin polarization anisotropy between the in-plane and out-of plane spin currents, expected from our band calculations.[19] However, this is difficult to confirm, since this difference in *P* can be due to larger errors in the measurements of the type *B* MnAs compared to the type *A*,[20] and may also arise from different microscopic structure of type *B* samples. A single crystal of bulk MnAs is needed to give a definitive answer to this important question.

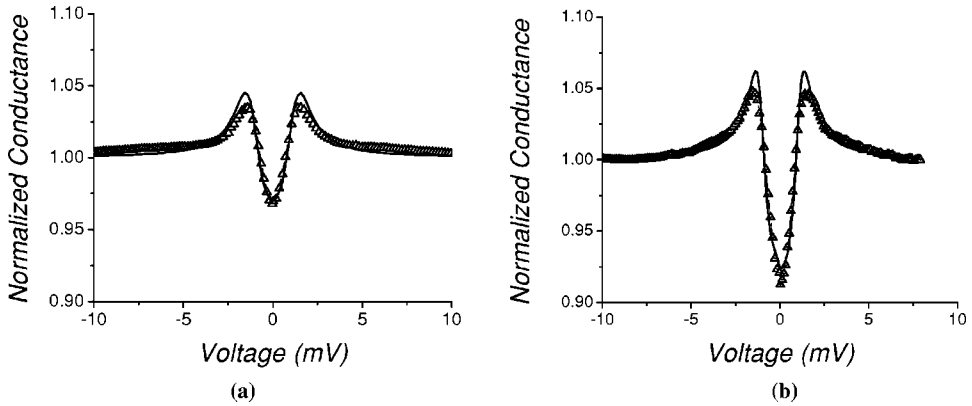

FIG. 2. Normalized conductance data fitted (solid curve) with the model of Ref. 12 at $T=1.2$ K. (a) Sn point contact with type *A* MnAs with contact resistance $R_c=37$ Ω from Fig. 1. Fitting parameters: $Z=0.1$, $P=51\%$. (b) Normalized conductance curve of a Pb point contact with type *B* MnAs and the corresponding fit with $Z=0.15$, $P=52\%$. No features were seen on the conductance curves above the critical temperatures of Sn and Pb (3.7 K and 7.2 K, respectively).

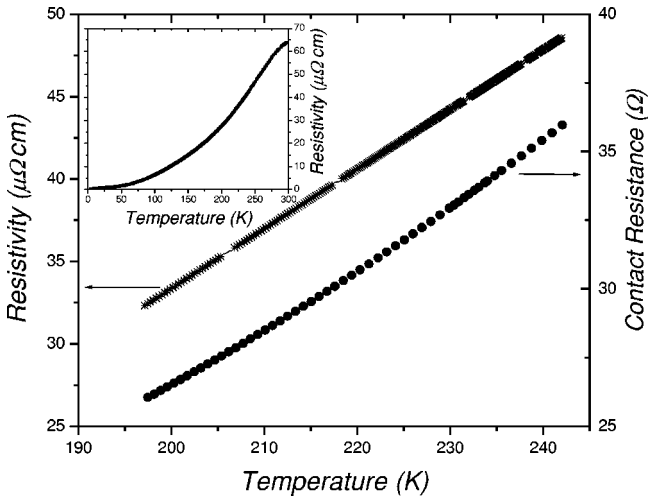

FIG. 3. Sn-MnAs point contact resistance of and in-plane resistivity data for the same sample of type *A* MnAs in the temperature range (~200–240 K) where both dependencies are approximately linear. Inset: Resistivity of MnAs between 4 K and 300 K.

We have independently determined the transport regime, by estimating the elastic mean free path L and the contact size d. We evaluate d from the temperature dependence of the contact resistance at zero bias $R_c(T)$ at high temperatures, where $R_c(T)$ is proportional to the resistivity $\rho(T)$ of MnAs film[21] (see Fig. 3). Then

$$d=\frac{d\rho/dT}{dR_c/dT}, \quad L=\frac{3\pi}{16}\left(\frac{R_c(0)d^2}{\rho}-d\right).$$

Our probe design allowed us to measure the temperature dependence of the contact in a broad temperature range. The estimates for MnAs type *A* film and Sn tip with the typical contact resistance $R_c \sim 10\ \Omega$ were done in the temperature range 200–245 K with $dR_c/dT=0.22\ \Omega$/K and $d\rho/dT=0.35\times10^{-6}\ \Omega$ cm/K, resulting in $d=15$ nm and $L=330$ nm. These estimates show that $L \gg d$, fully justifying the use of the ballistic formulas in the data analysis.

To check the integrity of our contacts, we have measured the phonon spectrum d^2I/dV^2 of lead in the superconducting state, which is proportional to the Eliashberg function $\alpha^2F(\varepsilon)$ (Fig 4). The observed spectral peaks, shifted to higher energies compared to the normal state, are very close to the known phonon peaks of Pb,[22] as well as to the ones obtained previously by the Cornell group.[10] The ability to see good phonon spectra is commonly associated with small impurity scattering within the contact area.[10] This gives us yet another confirmation of the ballistic nature of the contacts.

Additionally, we have performed band structure calculations of MnAs in the NiAs phase, using the Stuttgart Linear muffin-tin orbital (LMTO) tight-binding (TB) code and the generalized gradient approximation (GGA) approximation for the exchange-correlation potential.[23] The calculated band structure agrees with the previous results.[24] The Mn majority *d* band is almost fully occupied, and only As *p* bands cross the Fermi level for majority electrons, which are light and have sizable velocity. In the minority spin channel, the Fermi

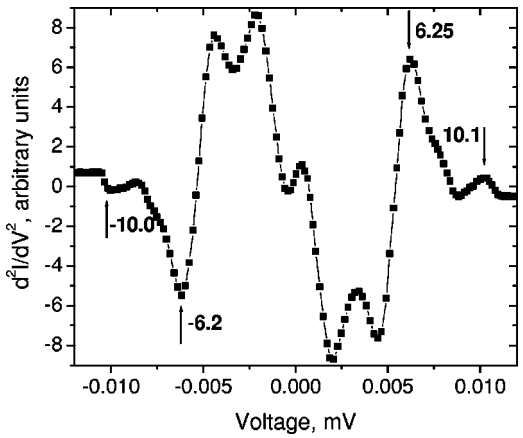

FIG. 4. Phonon spectra for Pb/MnAs (type *A*) junction. Upon subtracting the value of the superconducting gap Pb, the two peaks (at 4.65 and 8.8 mV) practically coincide with the tabulated peak values of the Eliashberg function of Pb (Ref. 22).

level lies in the Mn *d* band. The Fermi velocity in this channel is smaller, by approximately a factor of 4 (see Fig. 5). This is reminiscent of the 3*d* metals, such as Ni, and, similarly, leads to a *negative* density-of-states (DOS) polarization, but to a *positive* current.[25]

The calculations yield the spin polarization for density of states $P_0=-15\%$. For the ballistic transport in the plane perpendicular to the *c* axis of MnAs $P_{1\perp}=42\%$, and parallel to the *c* axis $P_{1\parallel}=15\%$. For diffusive (Ohmic) transport $P_{2\perp}=80\%$ and $P_{2\parallel}=43\%$. Importantly, this implies that 80% of the current in plane in the bulk of MnAs is transferred by the majority spins. The projection of the in-plane Fermi velocities onto the current direction for majority and minority spin channels are $\langle V_{F\uparrow}\rangle=4.3\times10^7$ cm/s, $\langle V_{F\downarrow}\rangle=1.1\times10^7$ cm/s, respectively. Our estimates of the mean free path L from the temperature dependence of the contact resistance above ($L=330$ nm) can be now cross-checked by calculating the conductance, $\sigma_i=e^2\langle N(E_F)V_{Fi}^2\rangle\tau$, where the

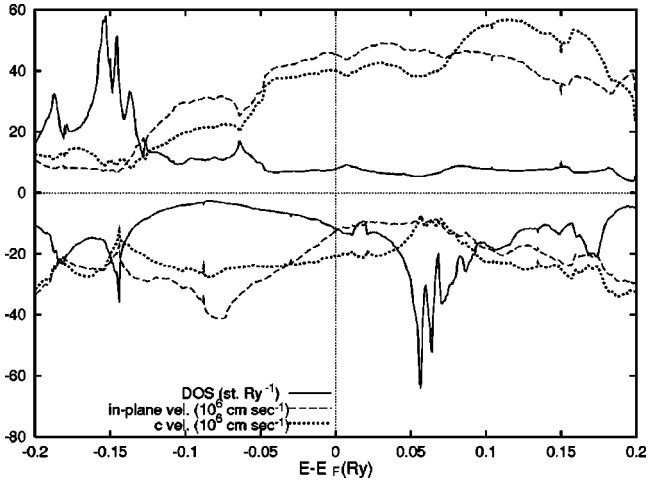

FIG. 5. Calculated densities of states (solid line, in states/Ry) and in-plane and *c*-axis electron velocities (dashed lines, in 10^6 cm/s) for spin-up and spin-down bands of MnAs (top and bottom panels, respectively).

relaxation time $\tau = L/\langle V_F \rangle \sim 8 \times 10^{-13}$ s. Using the calculated values $\langle N(E_F) V_{F\uparrow}^2 \rangle = 2.2$ Ry bohr^2 and $\langle N(E_F) V_{F\downarrow}^2 \rangle = 0.3$ Ry bohr^2 in plane we obtain $\langle N(E_F) V_F^2 \rangle = \langle N(E_F) V_{F\uparrow}^2 \rangle + \langle N(E_F) V_{F\downarrow}^2 \rangle = 2.5$ Ry bohr^2, yielding $\rho_0 \sim 0.25\ \mu\Omega$ cm for the low-temperature resistivity, which is close to the observed $\rho_0 \sim 0.4\ \mu\Omega$ cm.

In summary, we have measured the spin polarization of type *A* and type *B* MnAs epitaxial films grown on (001) GaAs using the PCAR technique. We conclude from the temperature dependence study of the contact resistance and the resistivity of MnAs that all the measured contacts were in the ballistic regime. This is further supported by the phonon spectrum of Pb, acquired simultaneously with the conductance measurements. The transport spin polarization was 49% for type *A* (in the hexagonal MnAs plane) and 44% for type *B* samples. The somewhat lower spin polarization measured for type *B* samples suggests the presence of the spin anisotropy. The results are in good agreement with our *ab initio* calculations, which give $P_{1\perp} = 42\%$ in the hexagonal plane. Our calculations also indicate that $P_{2\perp} = 80\%$ of the current in the hexagonal plane of MnAs is transferred by majority spins, further emphasizing the potential importance of this attractive material system for spintronics applications.

We thank D.N. Basov, A.G. Petukhov, and I. Zutic for discussions and L.E. Wenger for the use of magnetic measurement facility. This work was supported by DARPA through ONR Grant No. N00014-02-1-0886 and NSF career grant (B.N.) and ONR Grant Nos. N00014-99-1-0071, N00014-99-1-0716, and N00014-99-1-1093 (N.S.).

[1] P. C. van Son, H. van Kempen, and P. Wyder, Phys. Rev. Lett. **58**, 2271 (1987); G.Schmidt *et al.*, Phys. Rev. B **62**, R4790 (2000).

[2] E. I. Rashba, Phys. Rev. B **62**, R16267 (2000).

[3] S. H. Chun, S. J. Potashnik, K. C. Ku, P. Schiffer, and N. Samarth, Phys. Rev. B **66**, 100408 (2002).

[4] A. T. Hanbicki, B. T. Jonker, G. Itskos, G. Kioseoglou, and A. Petrou, Appl. Phys. Lett. **80**, 1240 (2002).

[5] M. Tanaka, J. P. Harbison, M. C. Park, Y. S. Park, T. Shin, and G. M. Rothberg, Appl. Phys. Lett. **65**, 1964 (1994).

[6] J. J. Berry, S. J. Potashnik, S. H. Chun, K. C. Ku, P. Schiffer, and N. Samarth, Phys. Rev. B **64**, 052408 (2001).

[7] J. G. Braden, J. S. Parker, P. Xiong, S. H. Chun, and N. Samarth, Phys. Rev. Lett. **91**, 056602 (2003); R. P. Panguluri *et al.* (unpublished).

[8] N. Suzuki, M. Shirai, T. Ogawa, and I. Kitagawa, J. Magn. Magn. Mater. **177**, 1383 (1998); S. Sanvito and N. A. Hill, Phys. Rev. B **62**, 15553 (2000); Y. J. Zhao *et al.*, *ibid.* **65**, 113202 (2002).

[9] R. J. Soulen, Jr., J. M. Byers, M. S. Osofsky, B. Nadgorny, T. Ambrose, S. F. Cheng, P. R. Broussard, C. T. Tanaka, J. Nowak, J. S. Moodera, A. Barry, and J. M. D. Coey, Science **282**, 85 (1998).

[10] S. K. Upadhyay, A. Palanisami, R. N. Louie, and R. A. Buhrman, Phys. Rev. Lett. **81**, 3247 (1998).

[11] M. J. M. de Jong and C. W. J. Beenakker, Phys. Rev. Lett. **74**, 1657 (1995).

[12] I. I. Mazin, A. A. Golubov, and B. Nadgorny, J. Appl. Phys. **89**, 7576 (2001).

[13] G. E. Blonder, M. Tinkham, and T. M. Klapwijk, Phys. Rev. B **25**, 4515 (1982).

[14] K. Xia, P. J. Kelly, G. E. W. Bauer, and I. Turek, Phys. Rev. Lett. **89**, 166603 (2002).

[15] I. Zutic and O. T. Vallls, Phys. Rev. B **61**, 1555 (2000).

[16] B. Nadgorny, I. I. Mazin, M. S. Osofsky, R. J. Soulen, Jr., P. Broussard, R. M. Stroud, D. J. Singh, V. G. Harris, A. Arsenov, and Ya. Mukovskii, Phys. Rev. B **63**, 184433 (2001).

[17] F. Schippan, G. Behme, L. Daweritz, K. H. Ploog, B. Dennis, K.-U. Neumann, and K. R. A. Ziebeck, J. Appl. Phys. **88**, 2766 (2000).

[18] Y. Ji Y, G. J. Strijkers, F. Y. Yang, C. L. Chien, J. M. Byers, A. Anguelouch, G. Xiao, and A. Gupta, Phys. Rev. Lett. **86**, 5585 (2001); C. H. Kant, O. Kurnosikov, A. T. Filip, P. LeClair, H. J. M. Swargen, and W. J. M. de Jonge, Phys. Rev. B **66**, 212403 (2002).

[19] P in is higher in the hexagonal MnAs plane than perpendicular to it. For type *A* MnAs the current is measured in-plane, while for type *B* it is measured at an angle of $\sim 23°$ to that plane.

[20] The smaller error in P for type *A* MnAs samples is to be expected because of their lower sensitivity to the current direction due to the high hexagonal plane symmetry.

[21] A. I. Akimenko, A. B. Verkin, N. M. Ponomarenko, and I. K. Yanson, Sov. J. Low Temp. Phys. **8**, 130 (1982).

[22] See A. V. Khotkevich and I. K. Yanson, *Atlas of Point Contact Spectra of Electron-Phonon Interactions in Metals* (Kluwer, Boston, 1995).

[23] J. P. Perdew and Y. Wang, Phys. Rev. B **45**, 13 244 (1992).

[24] K. Katoh, A. Yanase, and K. Motizuki, J. Magn. Magn. Mater. **54**, 959 (1986); P. M. Oppeneer, V. N. Antonov, T. Kraft, H. Eschrig, A. N. Yaresko, and A. Ya. Perlov, J. Appl. Phys. **80**, 1099 (1996); P. Ravindran, A. Delin, P. James, B. Johansson, J. M. Wills, R. Ahuja, and O. Eriksson, Phys. Rev. B **59**, 15 680 (1999).

[25] B. Nadgorny, R. Soulen, M. Osofsky, I. I. Mazin, G. Laprade, R. J. M. van de Veerdonk, A. A. Smits, S. F. Cheng, E. F. Skelton, and S. B. Qadri, Phys. Rev. B **61**, R3788 (2000).